Polymer Chemistry

Accepted Manuscript

ROYAL SOCIETY OF CHEMISTRY

www.rsc.org/polymers

Design of Polyhedral Oligomeric Silsesquioxane (POSS) Based Thermo-Responsive Amphiphilic Hybrid Copolymers for Thermally Denatured Protein Protection Applications

Zibiao Li [a,+], Beng H. Tan [a,+], Guorui Jin [a], Kai Li [a], Chaobin He [a,b,*]

[a] Institute of Materials Research and Engineering, A*STAR (Agency for Science, Technology and Research), 3 Research Link, Singapore 117602, Singapore

[b] Department of Materials Science and Engineering, National University of Singapore, Singapore 117574, Singapore.

*correspondence to msehc@nus.edu.sg or cb-he@imre.a-star.edu.sg

[+]both these authors have made an equal contribution to this work

Abstract:

A series of thermo-responsive amphiphilic hybrid copolymers with random brush-like structure were synthesized by copolymerizing hydrophilic poly(ethylene glycol) methacrylate (PEGMA) and hydrophobic polyhedral oligomeric silsesquioxanes methacrylate (POSSMA) together with temperature sensitive poly(propylene glycol) methacrylate (PPGMA) via atom transfer radical polymerization (ATRP). The resultant poly(PEGMA-PPGMA-POSSMA) (PEPS) hybrid copolymers possess lower critical solution temperature (LCST) in the range of 31-33ºC. Static and dynamic light scattering (SLS and DLS) studies show that micellar structures created by PEPS copolymer in aqueous media were core-shell and possessed a thick hydration layer. The presence of a small amount of POSS (3.1 wt%) in the PEPS copolymers lowers the CMC of the micelles at room temperature by one order of magnitude compared to samples without POSSMA (PEP). Incorporation of POSSMA also enhances the stability of the formed micelles, i.e. PEPS containing 6.7 wt% POSS exhibits constant hydrodynamic radius, R_h (~65 nm) and aggregation number, N_{agg} (~350) when temperature is varied from 20 - 70°C while PEP without POSS shows a large increase in both R_h and N_{agg} values. On the other hand, the change of R_g as temperature increases could be attributed to the PPG brushes adopting a more extended and compact conformation below and above LCST respectively. The thermo-responsiveness of PPG brushes in PEPS hybrid micelles were also exploited to mimic the natural GroEL-GroES chaperone functionalities for renaturation of thermally denatured proteins. Above LCST of PPG, the chaperone-like system comes into effect with hydrophobic PPG domains on the micelles surface, providing spontaneous capture and protection of the unfolded proteins thus inhibiting the undesired protein aggregations at elevated temperature. Upon cooling, PPG returns to its hydrophilic state, thereby inducing the release of the bound unfolded proteins. The renaturation process of the detached proteins is spontaneously accomplished by the presence of PEG and OH-groups in the micelle corona. The working mechanism and thermal denaturation protection effect were also investigated by DLS, SLS and circular dichroism (C.D.) spectroscopy. In the presence of PEPS hybrid micelles, the protection efficiencies for GFP, lipase and lysozyme that can be achieved during the heat-induced denaturation process are 81.4%, 89.3% and 88.7% respectively. Cell culture and cytotoxicity studies revealed that the PEPS hybrid micelles could be effectively internalized by C6 Glioma cells and possess good cell biocompatibility. These interesting findings open up new opportunities to exploit PEPS hybrid copolymers as artificial chaperone for protecting unfolded proteins from toxic aggregation under high temperatures.

Keywords: Hybrid copolymers, stimuli-responsive, polyhedral oligomeric silsesquioxane (POSS), self-assembly, protein protection.

1. Introduction

Amphiphilic stimuli-responsive Polyhedral oligomeric silsesquioxanes (POSS) based hybrid macromolecules have attracted significant interest because these polymers have the ability to adopt conformations specific to the conditions of the surrounding environment, and they may be potentially fabricated into smart materials for advanced biological applications.[1-6] POSS are the smallest possible silica particles that have a well-defined cage-like framework made of silicon and oxygen atoms linked together in a cubic formation. Different functional groups have been successfully attached to the silicon atoms in the nanocage corners and this has made POSS particularly useful for the preparation of POSS-polymer hybrids through covalent bonding.[6, 7] More interestingly, the strong aggregation tendency of the super hydrophobic POSS molecules can effectively control the motion of the polymer chain and induce the self-assembly of molecular aggregates in a controllable manner. For instance, Li et al. reported a POSS-PDMAEMA (poly(2-(dimethylamino) ethyl methacrylate) hybrid polymer that self-assembled into single micelles with the POSS heads forming a crystal core and the PDMAEMA chains stretching as a corona. The individual micelles further aggregated into a reversible complex micelle-on-micelle structure under external pH change.[8] Similarly, several research groups have reported POSS-containing hybrid poly(*t*-butyl acrylate) (P*t*BA) with tadpole-shaped, dumbbell-shaped, and random-distributed polymer structures. These hybrid polymers can self-assemble into various aggregates in aqueous solutions due to the powerful hydrophobic nature of POSS and their self-assemblies demonstrated pH-dependent sizes and morphologies.[9-11] Zheng and his co-workers discovered that the self-organized hydrophobic micro-domains formed by hybrid POSS-caped poly(ethylene glycol) (PEG) telechelics could facilitate a rapid de-swelling and re-swelling response of poly(N-isopropylacrylamide) (PNIPAAm)/POSS-PEG-POSS organic-inorganic thermogels.[12] Recently, our group has reported star-shaped POSS-PDMAEMA hybrid polymers consisting of PDMAEMA in the corner as efficient drug and gene co-delivery carrier. Due to the amphiphilic properties of POSS-PDMAEMA hybrid polymers, hydrophobic paclitaxel was able to encapsulate within the hydrophobic core and the synergistic effect of drug and gene promoted superior gene transfection efficiency than the polyplexes without drug loading.[5] Furthermore, PEG-P(POSSMA)

hybrid di- and triblock copolymer synthesized in our lab demonstrated interesting micelle formation behaviour in aqueous solution where the micelles tended to accommodate a larger number of copolymer chains at elevated temperatures.[13] Interestingly, higher concentrations (~8.8 wt%) of P(POSSMA)-PEG-P(POSSMA) triblock copolymer in water lead to a hydrogel formation, and the rheological performance can be further tuned by the addition of POSS nanoparticles and UV treatment.[6]

While PEG has been widely studied as a temperature responsive polymer, the high phase transition temperature of PEG makes it less desirable for biomedical applications.[14] On the other hand, poly(propylene glycol) (PPG) is also a thermally responsive polymer with tuneable hydrophilic-hydrophobic properties stimulated by external temperature. In addition, its phase transition temperature ranges from 14 °C to 100 °C, depending on the architecture and molecular weight, which makes it more attractive for a wide variety of applications.[15, 16] In this contribution, PPG methacrylate derivatives (PPGMA) are incorporated with POSSMA and PEGMA to obtain thermo-responsive random poly(PEGMA-PPGMA-POSSMA) (PEPS) hybrid copolymers that mimic the natural GroEL-GroES chaperone functionalities for refolding of thermally denatured proteins.[17] In non-physiological conditions, proteins are likely to permanently lose their biological functions when exposed to high temperatures, because of the lack of mechanisms that prevent unwanted proteins aggregation at high temperatures and failure to promote protein refolding into active conformation after heating.[18] The GroEL-GroES system has an interior barrel covered by some hydrophobic sites in the rim. These hydrophobic sites are used to capture unfolded proteins, thereby avoiding undesired aggregation. When triggered by adenosine 5'-triphophate (ATP), the hydrophobic binding sites in the barrel will be buried within the subunit interfaces, thus providing a hydrophilic environment that is favourable for refolding of the unfolded proteins.[17] The most classical system that has been reported to simulate the molecular chaperone functionalities is based on a two-step mechanism, which involves complicated capture-binding-stripper procedures through addition of various additives and tedious post-processing.[19-21] The capturer (hydrogels, nanoparticles or cationic copolymers) binds with the denatured proteins through hydrophobic or electrostatic interactions and prevents proteins from aggregating on heating. Then the

strippers (additives such as cyclodextrins or anionic poly(acrylic acid) (PAA)) are introduced to interrupt the interactions between the capturer and proteins thus releasing the refolded proteins. In contrast to the complicated classical methods, we hypothesize that our current thermo-responsive amphiphilic PEPS hybrid copolymer self-assemblies could function as an artificial chaperone to spontaneously capture unfolded proteins on reaching the denaturation temperature and release refolded proteins under proper cooling conditions by using easy-controllable temperature as the sole trigger in an "on-demand" fashion.

2. Experimental Section

2.1. Materials

Methacrylisobutyl-POSS (POSSMA) was purchased from Hybrid Plastic (Product No. MA0702) and used as received. Poly(propylene glycol) methacrylate (PPGMA, M_n = 375), Poly(ethylene glycol) methacrylate (PEGMA, M_n = 360 and 900), Ethyl 2-bromoisobutyrate (EBiB, 98%), 1,1,4,7,10,10-hexamethyltriethylenetetramine (HMTETA, 99%), copper(I) bromide (CuBr, 99%), triethylamine (>99%), 4-Nitrophenyl acetate (97%), Acetonitrile (99.8%), Micrococcus lysodeikticus ATCC No. 4698 and 2-propanol (>99.5%) were obtained from Sigma-Aldrich. Purified nitrogen was used in the polymerization reactions. Lipase from Pseudomonas cepacia (Sigma-Aldrich), Lysozyme from Chicken Egg White (Merck) and Green Fluorescent Protein (GFP, Merck) were used as model proteins in the activity assay.

2.2. Synthesis of Poly(PEGMA-PPGMA-POSSMA) (PEPS) Hybrid Copolymer by ATRP

Poly(PEGMA-PPGMA-POSSMA) hybrid copolymers derived from PEGMA, PPGMA and POSSMA are denoted as PEPS copolymers, where the first P represents poly-, E for PEGMA, the second P represents PPGMA, and S for POSSMA. The control copolymer, poly(PEGMA-PPGMA) without POSS is denoted as PEP. PEPS hybrid copolymers were synthesized by ATRP with the molar ratios of PEGMA/PPGMA fixed at 1:2 and POSSMA content ranging from 1.97 to 5.66 mol%. In a typical experiment, PEGMA (4.0 g, 11.1 mmol), PPGMA (8.3 g, 22.2 mmol), POSSMA (0.63 g, 0.67 mmol), EBiB (50 μL, 0.34 mmol), and HMTETA (184 μL, 0.68 mmol) were introduced into the flask containing

15 mL of 2-propanol. After the reactants were dissolved completely, oxygen was removed by repeated *vacuum-nitrogen-cycling* system. Then, the degassed CuBr in 1 mL 2-propanol was added into the flask under nitrogen atmosphere. The reactions were allowed to proceed under continuous stirring at 60 °C for a desired reaction time. The molecular weight was monitored by gel permeation chromatography (GPC) analysis. After polymerization, the solution was diluted with tetrahydrofuran (THF) and passed through a neutral aluminium oxide column to remove the copper catalyst. THF was removed under reduced pressure to give a concentrated solution. Products were precipitated in excess of hexane to remove free PPGMA and POSSMA. The precipitated mixture of PEPS copolymer and PEGMA was re-dissolved in deionized water and purified by dialysis (Spectrum dialysis membrane, MWCO 5000) for 72 h to remove free PEGMA using deionized water, which was changed regularly. Polymer samples were obtained after freeze-drying and weighed to obtain the final yields.

2.3. Characterization of PEPS Hybrid Copolymers

^{1}H-NMR spectra were recorded on a Bruker AV-400 NMR spectrometer at room temperature. The chemical shift at 7.3 ppm is attributed to the solvent peaks $CHCl_3$. GPC analysis was carried out with a Shimadzu SCL-10A and LC-8A system equipped with a Shimadzu RID-10A refractive index detector. THF was used as the eluent at a flow rate of 1.0 mL/min at 40°C. Monodisperse PMMA standards were used to obtain a calibration curve. Copolymer compositions in molar ratios were evaluated by the proton integral regions as assigned in Fig. 1. The weight fraction of POSS in the hybrid copolymers were determined by thermogravimetric analyses (TGA, TA Q500) and the results are tabulated in Table 1. Samples were heated at 10 °C/min to 700 °C under air at flow rate of 60 mL/min. Thermal responsive behavior of the copolymer solutions was performed by UV-Vis spectrophotometer (Agilent 8453) at 530 nm. Aqueous copolymer solutions at concentration of 2.0 mg/mL were used for the measurements with temperatures ranging from 20 to 70 °C. The onset temperatures determined from the derivative absorbance spectroscopy were defined as the lower critical solution temperatures (LCST) of the copolymer solutions.

2.4. Self-assembly Behavior of PEPS Hybrid Copolymer Solutions

Dynamic Light Scattering (DLS) measurements were made with a Brookhaven BI-200SM multi-angle goniometer equipped with a BI-APD detector. The light source was a 35 mW He-Ne laser emitting vertically polarized light of 632.8 nm wavelength. From the expression $\Gamma = D_{app} q^2$, the apparent translational diffusion coefficients, D_{app}, were determined where Γ is the decay rate and q is the scattering vector. The apparent hydrodynamic radius, R_h can be determined by the Stokes-Einstein relationship:[22, 23] $R_h = \frac{kT}{6\pi\eta D_{app}}$, where k, η and T are the Boltzmann constant, viscosity of solvent, and the absolute temperature, respectively. The sample temperature was equilibrated for 30 minutes before the measurement was made. The scattering intensity of each concentration of the copolymer in deionized water was measured and plotted against the polymer concentration. The concentration at which the scattering intensity increases sharply was defined as the critical micelle concentration, CMC.

Static light scattering (SLS) measurements were performed to determine the weight-average molecular weight (M_w), z-average radii of gyration (R_g), and second virial coefficients (A_2) of the micelles in aqueous solution according to the relation; $\frac{Kc}{\Delta R_\theta} = \frac{1}{M_w}[1 + \frac{q^2 R_g^2}{3}] + 2A_2 c$, where K is the optical constant, which depends on the refractive index increment (dn/dc) of the polymer solution, c is the concentration of the polymer solution and ΔR_θ is the excess Rayleigh ratio.[24, 25] The scattering angles ranged from 50° to 120° at 10° intervals while the copolymer concentration ranged from 0.5 to 1.0 mg/mL. The refractive index increment (dn/dc) of each copolymer solution was measured using a BI-DNDC differential refractometer at a wavelength of 620 nm. The instrument was calibrated primarily with potassium chloride (KCl) in aqueous solution.

The particles aggregation morphologies were recorded on a high-resolution transmission electron microscope (Philips CM300 FEGTEM) (TEM) operated at accelerating voltage of 300 kV. Samples were prepared by depositing one drop of the copolymer solution (0.5 mg/mL) onto 200 mesh copper grids, which were coated in advance with supportive Formvar films and carbon (Agar Scientific). The samples were kept for 24 h at 25°C and 70 °C prior to TEM imaging.

2.5. Thermally Denatured Protein Protection Efficiency Assay

Three representative proteins, GFP, lipase and lysozyme that can undergo thermally induced denaturation procedure were carried out in this study. Samples were prepared by mixing the copolymer micelle solutions with each protein solution at known concentrations, and the protection efficiencies were evaluated according to the previously reported methods with minor modifications as stated in S1.2.[26-28]

2.6. Far-UV Circular Dichroism Analysis

The far-UV circular dichroism spectrum (C.D.) was recorded with a J-720 C.D. spectrophotometer (JASCO Co., Ltd., Tokyo, Japan) equipped with a thermo-regulated cell compartment. The change in the C.D. ellipticity of proteins with and without PEPS copolymers in phosphate buffer (pH 7.2) was measured.

2.7. Cellular Uptake and Cytotoxicity Assay

The cellular uptake of the prepared copolymer micelles by the C6 Glioma cells (ATCC, USA) was investigated by confocal laser scanning microscopy FV1000 (CLSM, Olympus Japan) using the green fluorescence in GFP as probe (S1.3).[29] After 24 h incubation, the cell monolayer was fixed and imaged by CLSM under the same experimental conditions.[30] The *in vitro* cytotoxicity of PEPS hybrid copolymers were carried out using MTT assay in metabolic activity of human dermal fibroblasts (HDFs) cell lines (S1.3). The relative cell viability (%) was calculated from the absorbance ratios of the formazan products at 570 nm.[31] All experiments were conducted with six repetitions and averaged.

3. Results and Discussion

3.1. Synthesis and Characterization of PEPS Hybrid Copolymers

Previously, we reported the synthesis of amphiphilic di-, and tri- block copolymers consisting of PEG and POSS derivatives, and investigated their tuneable self-assemblies in both micelle and hydrogel formations in aqueous solutions.[6, 32] However, in the current study, a random brush-type thermo-responsive PEPS hybrid copolymers derived from methacrylate of PEG, PPG, and POSS were designed to mimic the natural chaperone for thermally denatured protein protection applications. PEPS hybrid copolymers were prepared by ATRP using ethyl 2-bromoisobutyrate as initiator. The synthetic route and

schematic illustration of the random brush-type PEPS hybrid copolymers in this paper are presented in Scheme 1. By varying the feed content of POSSMA from 1.96 to 5.67 mol%, a series of PEPS hybrid copolymers were synthesized, and its counterpart, poly(PEGMA-PPGMA) (PEP) copolymer without POSS were prepared for structure-property relationship studies. The chemical structure of PEPS hybrid copolymers were verified by ^{1}H NMR spectroscopy. Fig. 1 shows the typical ^{1}H NMR spectrum of PEPS-3 in $CDCl_3$, in which all proton signals belonging to PEG, PPG, POSS, and poly(methacrylate) segments are confirmed. The signals at 3.6 ppm are assigned to the –CH_2–CH_2–O– of PEG, signals corresponding to –OCH_2– in repeated units of PPG segments are observed at 3.25 ppm, and the signals at 0.58 – 0.60 ppm are associated with methylene protons (f and g in Fig. 1) of POSSMA.[32-34] Protons in –CH_3– and –CH_2– of the poly(methacrylate) backbone in PEPS copolymers are identified at δ ~ 0.95 – 1.1 ppm and δ ~ 1.8 – 2.0 ppm, respectively. However, resonances observed at δ ~ 5.75 and 6.2 ppm for vinyl protons in all the starting materials are not shown in the final products, indicating that the copolymerization of the three components has successfully occurred, and PEPS hybrid copolymers with high purity was obtained. The composition of the final PEPS hybrid copolymer in molar ratio, represented by *x*, *y*, and *z* values in the macromolecule structure (Fig. 1), was estimated by comparing the integral values of the corresponding signals, according to Eqs. (1), (2) and (3) (S1.1).[35] The data was summarized in Table 1. The molar ratios of PEG/PPG in the final polymer determined from NMR spectra is larger compared to the feed ratio of 1:2, as demonstrated in Table 1, which is attributed to the higher reactivity of the vinyl groups in PEGMA as compared to the vinyl groups in PPGMA. The lower reactivity of the vinyl groups in PPGMA is due to the steric hindrance of methyl group located in PPG segments which agrees with previous studies on the copolymerization of PEG and PPG containing macromolecules as *in situ* thermogels.[35, 36] Further verification of the successful synthesis of PEPS hybrid copolymers is obtained from GPC analyses where the copolymers synthesized in this paper have high molecular weight (2.01×10^4–2.56×10^4 g/mol) and low polydispersity (1.41−1.56) as presented in Table 1. Fig. 2 shows the representative GPC profiles of PEPS hybrid copolymer and its precursors where all the traces show a monomodal peak of the molecular weight distribution, revealing the high purity of the tested samples rather than a mixture. In addition, PEPS copolymer trace shows a higher

molecular weight (shorter elution time) as compared to the traces of the starting materials. The concomitant increase in the molecular weight, together with the NMR results of the copolymers indicates that the copolymerization was successful.

The PEPS hybrid copolymers were subjected to thermal gravimetric analysis (TGA) and the representative TGA curves are shown in Fig. 3. PPGMA and PEGMA prepolymers were completely decomposed at c.a. 500 °C under air atmosphere (Fig. 3, curves c and d). In addition, the residual in Fig. 3 (curve a) indicates that the organic ligand of POSSMA have completely decomposed at elevated temperature above 500 °C; *i.e.,* the POSS segments were transformed into ceramics due to thermal decomposition and oxidation. Therefore, the ceramic yields can be employed to estimate the content of POSS in PEPS hybrid copolymers and the results are summarized in Table 1.[12] The ceramic yields were measured to be 3.1, 6.7, and 6.3 wt % for PEPS-1, PEPS-2 and PEPS-3 hybrid copolymers, respectively, which is quite close to the ceramic yields calculated in terms of the molar ratios. The TGA results further confirmed the as-synthesized PEPS copolymers in hybrid compositions.

UV-Vis spectrophotometer was used to characterize the thermo-responsive behaviors of PEPS hybrid copolymers by measuring the optical absorbance of the copolymer solutions (2.0 mg/mL) as a function of temperature as demonstrated in Fig. 4(a). The temperature at which the absorbance increases sharply is defined as the lower critical solution temperature (LCST). The first derivative absorbance plot, which reflects the quantitative measurement of the sharp phase transition of the aqueous copolymer solution as a function of temperature, is shown in Fig. 4(b) and the LCST values determined from this method are tabulated in Table 1. The aqueous solutions of PEPS copolymers exhibit LCST that is very similar to the poly(N-isopropylacrylamide) (PNIPAAm).[37, 38] From Table 1, the LCST of PEP copolymer solution is 29.0 °C, that is, at temperatures below LCST, PPG is a hydrophilic water-soluble polymer and PEP copolymer solution is clear with very low optical absorbance. Above this temperature, PPG becomes hydrophobic and collapses to form larger aggregates, leading to a turbid solution with increased absorbance (Fig. 4(a)). The continuous decrease in absorbance beyond the LCST of PEP copolymer solution is due to the precipitation of larger aggregates.[36] In contrast, at similar PEG/PPG ratio, the

incorporation of hydrophobic POSS in PEPS-1 and PEPS-2 hybrid copolymer solutions exhibit improved thermal stability, as seen from the flat absorbance curves at the same elevated temperature range (beyond the LCST) as depicted in Fig. 4(a). Moreover, the LCST for these two hybrid copolymers, PEPS-1 and PEPS-2, are higher compared to that of PEP copolymer without POSS (Fig. 4(b) and Table 1). When the POSS content in PEPS is 3.1 wt% (PEPS-1) and subsequently increased to 6.7 wt% (PEPS-2), the LCST increases to 31 ºC and 33 ºC respectively. The effect of POSS on the LCST of the PEPS copolymers is consistent with the previously reported PNIPAAm-PLA-PNIPAAm copolymers where we demonstrated that the LCST of PNIPAAM in water could be tailored from 32 ºC up to 38.5 ºC by increasing the PLA content in the copolymers or forming more hydrophobic stereocomplexes between enantiomeric PLA segments.[39] These observations are due to the changes in the polymer-solvent interactions arising from the changes in the hydrophilic/hydrophobic balance of the copolymers.[36, 40] In the case of PPG in water, hydrogen bonding occurs between the water molecules and the oxygen atoms of PPG, resulting in a negative entropy. Increasing the POSS content in the copolymers would result in an increase in the inter-polymer interaction in aqueous solution and subsequently a more negative entropy. According to the Flory-Huggins solution theory, temperature has to increase in order to negate enthalpy change and make the overall Gibbs free energy positive.[39, 41] However, the macroscopic phase transition of PEPS-3 copolymer solution from clear to turbid was not observed in the experimental temperature range, because the longer PEG brushes in PEPS-3 could provide superior water solubility of the copolymer than its counterparts. The abrupt increase in absorbance at above 60 ºC is probably due to the PEG dehydration and subsequent association (Fig. 1S).[36, 42] Thermo-responsiveness studies show that the incorporation of POSS in PEPS hybrid copolymer could afford better thermal stability of the copolymer solution, and the LCST can be adjusted by tuning the copolymer compositions.

3.2. Self-assembly of PEPS Hybrid Copolymer in Aqueous Solution

Micelles with P(MA-POSS) segments as the core and PEG and PPG brushes as the corona are expected to form in aqueous solution. DLS was used to determine the critical micelle concentration (CMC) of the PEP and PEPS copolymers in aqueous solution at different temperatures as shown in Fig. 2S(a) and (b). All the four samples display a similar trend in the CMC with increasing temperatures where the CMC

values remain quite constant below 30 °C and begin to show a decrease when temperature is increased up to approximately 38 °C, beyond which the CMC becomes quite constant again. The region which displays a decrease in CMC is consistent with the LCST of the copolymers (as depicted in Fig. 4) and can be explained as the region where PPG brushes undergo a phase transition due to decreased hydrogen bond interaction with water beyond LCST. Below 30 °C, PEP copolymer without POSS possesses high CMC values (~ 3mg/mL) and the CMC values decreases by almost two orders of magnitude when the temperature is increased up to 70 °C. With the presence of a small amount of POSS (3.1 wt%) in the copolymers, the CMC values are lowered as depicted in PEPS-1, as compared to samples without POSS. In addition, the CMC values decreases further with increasing POSS content in the copolymers (see PEPS-2) suggesting that the higher POSS content favours micellization promoted by an increased in hydrophobicity. It is also interesting to note that the decrease in CMC values is more gradual for copolymers with POSS (PEPS-1, PEPS-2 and PEPS-3) when temperature is increased from 20 to 70 °C (e.g., 0.3mg/mL to 0.1mg/mL for PEPS-1) as compared to sample without POSS (PEP) which decreases almost two orders of magnitude for the same temperature range. We hypothesized that the presence of POSS plays a part in formation of a more stable micelle in aqueous solution. When comparing the effect of PEG content in the copolymers (PEPS-2 and PEPS-3), sample with larger PEG content possesses higher CMC values for the same temperature range due to the increased hydrophilicity of the copolymers resulting in unfavourable micelle formation in aqueous solution.

The hydrodynamic radius, R_h of the micelles in aqueous solution formed by the PEP and PEPS copolymers at different temperatures were measured using DLS for copolymer concentrations ranging from 0.5 to 1.0 mg/mL, well above the CMC of PEPS-1 and PEPS-2, to ensure the micelle formation. Note that we attempted to measure the R_h of all samples at polymer concentration of approximately 3 mg/mL, to ensure micelle formation in all the PEPS and PEP samples throughout the whole temperature range of 20 to 70 °C (since the CMC of PEP is approximately 3 mg/mL at low temperatures). However, samples at this relatively high concentration (3 mg/mL) became very turbid when the temperature is increased beyond 30 °C resulting in very large light scattering intensities and hence inaccurate micelle size measurements. Therefore, the polymer concentrations of PEPS-1, PEPS-2 and PEP (at temperatures

above 30 °C) is kept below 1 mg/mL to ensure formation of micelle solutions which are clear to slightly translucent throughout the temperature range of interest. Fig. 5(a) and (b) demonstrate the particle size distribution of the micelles formed from PEPS-1 and PEPS-2 respectively for temperature ranging from 20 to 70 °C. The distribution is unimodal and becomes narrower when temperature is increased beyond ~33 to 35°C, depending on the sample. In addition, the dependence of decay rate Γ(the reciprocal of relaxation time, τ) on q^2 (according to $\Gamma = D_{app} q^2$), shown in Fig. 5(c), exhibits a linearity confirming that the observed peaks in Fig. 5(a) and (b) originate from the translational diffusion of the copolymer micelles.[23] The R_h at peak maximum of the PEP and PEPS micelles at each temperature is plotted as a function of temperature as depicted in Fig. 5(d) for copolymer concentration of 0.5 mg/mL. However, there are exceptions for PEP at temperatures below 30 °C (copolymer concentration of 4 mg/mL) and PEPS-3 (copolymer concentration of 2 mg/mL) due to the large CMC values of these samples (refer to Fig. 2S(b) and the discussion in the paragraph above). When comparing the effect of POSS content in the copolymers (see PEP, PEPS-1 and PEPS-2), as anticipated, PEPS-2, having the highest POSS content in the copolymer (highest hydrophobicity), formed the largest micelles (R_h ~ 65nm) in aqueous solution at temperatures below 30 °C as compared to PEP and PEPS-1. PEPS-1 formed micelles having R_h of approximately 20 nm which gradually increased to approximately 45 nm when the temperature is increased up to 40 °C, beyond which the R_h remained quite constant. PEP also formed micelles having similar R_h (~20 nm) at low temperatures but increases drastically to approximately 120 nm at temperatures above 30 °C. Interestingly, although both PEP and PEPS-1 has similar PEGMA and PPGMA content in the copolymer but without POSS in PEP, the formation of large micelles in PEP (R_h ~120 nm) at high temperatures, which is three times the size of micelles formed from PEPS-1 (R_h ~40 nm), can be attributed to the aggregation of a large number of micelles (inter micellar aggregation) due to the increasing hydrophobicity and instability of the micelle with increasing solution temperature. Instead, the milder increase in R_h observed in PEPS-1 with increasing temperature, suggests the enhancement of the stability of the micelles formed when POSS is present in the copolymers, which reduces the tendency to form inter micellar aggregates. In a similar manner, the R_h of PEPS-2 remained almost constant at

approximately 65 nm when temperature is increased from 20 to 70 °C further suggesting the formation of a more stable micelle in aqueous solution when a higher amount of POSS is present in the copolymer which prevents inter micellar aggregation at higher temperatures. From the TEM micrographs in Fig. 3S, spherical particles were observed and the estimated diameters were in good agreement with the size obtained using DLS at the two different temperatures. In addition to the effect of POSS content in the copolymers, we also investigated the effect of the length of the PEG brushes in the copolymers (see PEPS-2 and PEPS-3) on the micelle size. Similar to PEPS-2, the R_h of PEPS-3 remained almost constant at approximately 50 nm in the same temperature range further confirming that ~6wt% POSS content in the copolymer is sufficient for the formation of stable micelles in aqueous solution. The micelle size obtained from PEPS-3 is smaller compared to PEPS-2 due to the longer PEG brushes in the former, which reduces the hydrophobicity and tendency to form micelle leading to formation of smaller micelles in PEPS-3. Nevertheless, the stability of the micelle was not compromised with the incorporation of a longer PEG brush length as the micelle size remained constant throughout the whole temperature range investigated.

Static light scattering (SLS) experiments was further used to elucidate the effect of temperature and POSS content in the copolymers on the aggregation of the PEP and PEPS copolymers in solution. The apparent molecular weight of the micelle ($M_{w,micelle}$), together with the radius of gyration (R_g) were determined by a Zimm plot in SLS as a function of temperature. Note that the $M_{w,agg}$ values in aqueous solutions are much larger than the $M_{w,single}$ values of the individual PEP and PEPS copolymers obtained by GPC, further confirming the formation of PEP and PEPS micelles in aqueous solution. Subsequently the apparent aggregation number, N_{agg} ($N_{agg} = M_{w,micelle}/M_{w,single}$) of the micelles in aqueous solution were calculated as depicted in Fig. 6(a) where the trend is quite similar to the hydrodynamic radius as a function of temperature (Fig. 5(d)). Below 30 °C, the N_{agg} appears to be quite constant at approximately 40 and 65 for PEP and PEPS-1 respectively. When the solutions were further heated to 37 °C, there is an increase in the N_{agg} where the increment is larger in PEP (~450) compared to PEPS-1 (~85) which further confirms our hypothesis that the micelles formed from the PEP becomes highly instable with increasing solution temperature and the stability of these micelles can be enhanced with the incorporation of

sufficient POSS in the copolymers as observed from the smaller increment in N_{agg} for PEPS-1 and subsequently stable N_{agg} in PEPS-2 and PEPS-3. In addition, samples with larger amount of POSS formed micelles with higher N_{agg} (comparing PEPS-1 and PEPS-2) and the N_{agg} reduced when a longer PEG segment is incorporated in the copolymer (comparing PEPS-2 and PEPS-3) which complements our particle size data that the tendency to form micelles increases when the amount of POSS is increased and the length of the PEG is reduced in the copolymer.

In addition to the $M_{w,micelle}$ and N_{agg}, the dimensionless ratio R_g/R_h which is indicative of the aggregate structure,[43, 44] ranges from 0.25 to 0.45 for the copolymer micelles at temperatures below 30°C, as depicted in Fig. 6(b). The values of R_g/R_h for hard-sphere micelle, random coil, and rod-like structure are reported as 0.78, 1.78, and ≥2, respectively.[43, 44] The deviation of R_g/R_h of our PEP and PEPS copolymer systems from the hard sphere value suggests that the micelles are spherical in shape and possess a thick hydration layer (core-shell aggregate structure). When comparing the PEP and PEPS copolymers below the LCST, the high hydrophobicity of POSS nanocages in PEPS hybrid copolymers provides stronger driving force for self-assembly and larger micelles cores were formed in aqueous solution as manifested by the larger R_g/R_h values as compared to micelles from PEP copolymers. When the temperature of the samples were increased above the LCST, the R_g/R_h experienced a slight but significant increase (ranging from 0.05 to 0.3, depending on the sample) while maintaining the spherical shape of the micelles as indicated by the values of $R_g/R_h < 0.78$. Above the LCST, PPG experienced a phase transition due to decreased hydrogen bond interaction with water leading to its collapsed towards the core of the aggregates which is consistent with the increased in R_g/R_h. The increase in R_g/R_h is smaller in samples with larger amount of POSS and shorter PEG. For example the R_g/R_h ratio increases from 0.3 to 0.65 in PEP copolymer when temperature is below and above LCST respectively as compared to the increase from 0.44 to 0.54 in PEPS-2 copolymer for the same temperature range. This observation suggests that in the presence of POSS nanocages in the PEPS micelles, PPG brushes collapses and forms a compact hydrophobic layer surrounding the POSS core when temperature is increased above the LCST, resulting in a small increase in R_g/R_h. In contrast, the collapse of the PPG brushes in the loosely packed PEP micelles increases the tendency to self-assemble and reduces the micelle stability in aqueous solution, as

reflected by the large increase in particle size above the LCST. As a consequence, the hydrophobic domains formed from PPG phase transition are entrapped in the PEP micelles cores through intermicellar aggregations and are less compact, as suggested by the R_g/R_h ratio. To summarize, the constant R_h and N_{agg} of micelles (Figs. 5(d) and 6(a)) and the increased in R_g/R_h ratios (Fig. 6(b)) observed in PEPS-2 and PEPS-3 when temperature is increased above LCST implies that stable aggregates are formed in aqueous solution when sufficient POSS nanocages are present in the copolymers and that the change in R_g as a function of temperature is purely due to the PPG brushes adopting a more extended and compact conformation below and above LCST respectively.

3.3. Thermally Denatured Protein Protection of PEPS Hybrid Copolymers Micelles

The chaperone role of the as-prepared PEPS hybrid micelles in the thermally denatured protein protection was investigated by monitoring the recovered protein and enzyme activity in the presence of the micelles. Three representative proteins GFP, lipase, and lysozyme were used in the measurements and the protection efficiencies in the presence of different copolymer concentrations are shown in Fig. 7. During the measurements, the solutions were heated at 70 °C and kept at this temperature for 30 min to denature the three proteins. It is well known that, without any external assistance, these proteins will irreversibly lose their activities as a result of the aggregation of the denatured intermediates.[32-34] In our measurements, the relative residual activities of the three representative free proteins were found at 22.4%, 42.1%, and 40% for GFP, lipase and lysozyme, respectively (Fig. 7). However, in the presence of the PEPS hybrid micelles, all the proteins activities were well protected after going through the harsh heat-deactivation procedure. For example, at the two tested copolymer/protein ratios, the optimal protection efficiency of GFP was observed to be 81.4%. Moreover, 89.3% and 88.7% of the enzyme activities of lipase and lysozyme, respectively, were recovered in the presence of PEPS hybrid copolymer at concentration of 2.0 mg/mL. These results clearly indicate that the irreversible aggregations of the denatured proteins were inhibited and, more importantly, the native functional conformation could be recovered from the denatured state. The relatively low protection efficiency of PEPS-3 hybrid micelles were probably caused by the longer PEG brushes in the exterior phase of the micelles, which are reported to be unfavorable for the protein absorption during the unfolded protein capture.[41] Comparing the PEP

and PEPS copolymers, the decreased in protein protection efficiency in the case of PEP copolymer may be attributed to the slightly different micelle formations in aqueous solution at elevated temperatures as discussed in Figs. 5(d) and 6. When temperature is increased above the LCST, PPG brushes collapses and forms a compact shell on the POSS core in the PEPS micelles, in contrast to the loosely packed PPG domains entrapped in the PEP micellar cores formed through intermicellar aggregations. As a consequence, there exists a larger hydrophobic area for protein capture and higher protection efficiencies were observed in the PEPS micelles as compared to the PEP micelles. The schematic representation of the self-assembly of PEPS hybrid copolymers in aqueous solution is presented in Fig. 8(A).

For thermally denatured proteins, the denaturation process is usually considered to occur by a two-step mechanism, as shown in Fig. 8(B). The folding, unfolding, and aggregation status presented in Fig. 8(B) depicts the native, reversibly denatured, and irreversibly denatured forms of proteins respectively. The thermal inactivation starts with reversible denaturation of protein which often proceeds to form inactive and insoluble aggregates driven by intermolecular associations.[18] This aggregation process is irreversible, which prevents proteins from refolding into their native stage and thus losing their functionalities.[27] However, the protein in the reversibly denatured form can be promptly protected through capture thus avoiding the irreversible aggregation. More importantly, the captured proteins could be refolded into the native functional conformation under proper conditions. The proposed mechanism of the PEPS hybrid micelles in protein protection is demonstrated in Fig. 8(c). Under normal conditions, the micelles self-assembled from PEPS hybrid copolymers are in the dormant state and do not interfere with the protein activities at temperatures below LCST. When the micelle solutions are heated to 40 °C, which is above the copolymers' LCST (31 - 33 °C) but below the unfolding temperature of proteins (~70°C), the micelles transform into their functional state due to the collapse of PPG polymer brushes in the mixed corona (step 1). The collapsed PPG polymers form hydrophobic domains on micelle cores made from POSS nanocages and poly(methacrylate) backbones, leaving behind cavity-like spaces that could accommodate the denatured proteins in step 2. Further increasing the temperature induces the denaturation of protein into unfolded intermediates and exposing the hydrophobic inner core of the

proteins. The unfolded intermediates are immediately captured through multipoint hydrophobic interactions with the hydrophobic domains of the micelles before protein aggregation could occur, resulting in the formation of micelle/protein complexes (step 3) and protection of the unfolded intermediates. The stretched PEG brushes in the outer layer could make the micelle/protein complexes stable and provide steric repulsion to prevent further intermicellar aggregation. Upon cooling, the micelle/protein complexes gradually dissociate, owing to the temperature sensitive phase transition of PPG brushes from hydrophobic to hydrophilic state, during which the unfolded intermediates detach from the micelles surfaces and start to refold into their native conformation (step 4). The presence of PEG brushes and hydroxyl groups in the mixed micelle corona could interact with the molten globules of the refolding intermediates, which could further enhance the protein renaturation.[45, 46]

The capture and release mechanism between the unfolded intermediates of the proteins and PEPS hybrid micelles was further confirmed by light scattering studies as summarized in Table 2. The radius of gyration, R_g and hydrodynamic radius, R_h of PEPS micelle/protein mixtures at 25 °C and 37 °C are similar to the PEPS micelles alone. However, after incubating at 70 °C for 30 min, the R_g, R_h and R_g/R_h values increased significantly, thus indicating that the interaction between micelles and proteins occurred to form micelle/protein complexes. The increase in R_g/R_h ratios at 70 °C in the micelle/protein complex demonstrates that the protein absorption and capture occurs mainly in the core (hydrophobic domain) of the PEPS micelles. The capture and holding of proteins in the micelles hydrophobic domains could effectively prevent the irreversible aggregation of the proteins. In addition, the light scattering data summarized in Table 2 demonstrates that the PEPS hybrid micelles returned to its original size range when cooled to room temperature (25 °C) indicating the disassembly of micelle/protein complexes as induced by the PPG phase transition into hydrophilic state. The above results confirmed the capture-and-release mechanism in the chaperone-like functionalities of PEPS hybrid micelles during the denaturation and renaturation of proteins. The protein protection effect arising from micelle/protein complexation was further investigated with far-UV circular dichroism (C.D.) spectra by monitoring the secondary structure of proteins at different conditions. Taking PEPS-1 hybrid micelle solution with lipase as an example, the

C.D. spectra of lipase did not change upon mixing with the copolymer, indicating that the presence of PEPS hybrid micelles did not perturb the structural integrity of lipase and there were no interactions between lipase and PEPS hybrid micelles at room temperature (Fig. 4SA). During the heat-induced denaturation process, the thermal aggregation temperature of free lipase was approximately 70 °C and this temperature was largely retarded (~82 °C) upon the formation of micelle/protein complexes, indicating higher stability of lipase in PEPS hybrid copolymer/protein mixed solutions (Fig. 4SB).

3.4. Cellular Uptake and Cytotoxicity Assay

The cellular uptake of the micelles was investigated by directly dissolving PEPS hybrid copolymers into C6 Glioma cell culture medium containing high concentration of GFP for efficient protein encapsulation.[47] As a control, free GFP in fresh DMEM was added into the cell culture chambers without the hybrid copolymers. Intrinsic fluorescence of GFP was used as probe to evaluate the cell uptake efficiency, by observing the fluorescence intensity of the cells under confocal laser scanning microscopy.[29, 48] As shown in Fig. 9A, after a 24 h incubation of the C6 Glioma cells with free GFP solution, only a few fluorescence signals were detected and most of the proteins were present as aggregates on the cellular membrane, indicating poor uptake of the proteins by the cells.[29] In comparison, when the cells were exposed to the same concentration of GFP but mixed with PEP copolymer solution, the GFP fluorescence intensity inside the cells was significantly enhanced (Fig. 9B), indicating an increased internalization of GFP in cells driven by PEP copolymer as delivery carrier. More interestingly, the cells incubated with PEPS-1/GFP mixed solution recorded the strongest emission signal (Fig. 9C, green channel), which suggests that the presence of POSS in the hybrid PEPS produced micelles that are more attractive to the cells for ingestion resulting in higher amount of GFP being delivered into the cells. We hypothesized that the PEPS hybrid micelles are more favorable for cell uptake due to its smaller micelle size as compared to micelles formed from the PEP copolymer. An overlay of the phase contrast image corresponding to the whole cell morphology and the bright green fluorescence of GFP indicates that the GFP has most likely localized in the cell cytoplasm (Fig. 9 Overlay). Therefore, the PEPS hybrid micelles could be effectively taken up by cells making it potentially useful as a delivery vehicle.

The cytotoxicity of the copolymer dissolved in cell culture medium was evaluated by incubating the medium with human dermal fibroblasts (HDFs) cells for a period of 48 h and 72 h, both at 37 °C. The cell viability at different time intervals was determined using the MTT assay and the results are shown in the supporting information (Fig. 5S). The cells showed no loss in cell viability when incubated for 48 h with both PEP and PEPS hybrid copolymers at concentration of 1.0 mg/m. Even at longer incubation time of 72 h and higher polymer concentration of up to 4.0 mg/mL, no effect of the polymer presence on cytotoxicity was observed. Therefore, based on the MTT assay, it is predicted that the PEPS hybrid copolymers developed in this paper are safe for biomedical applications.

4. Conclusion

Thermo-responsive PEPS hybrid copolymers were designed and their nano-scale micelle self-assemblies in aqueous solution was fabricated to functionalize as an artificial molecular chaperone for effective protein protection in the thermal-induced denaturation process. With the presence of POSS, the resulting PEPS hybrid copolymers solution showed stronger self-assembly tendency and better thermal stability in comparison to PEP copolymers without POSS. At the functional state, the dehydrated PPG brushes on the PEPS micelle surface collapsed to form hydrophobic domains, which can be used to spontaneously capture and protect the unfolded proteins intermediates at elevated temperature, thus preventing undesirable protein aggregation. During cooling, the temperature-sensitive PPG brushes returned to their hydrophilic state, thereby inducing the release of the bound unfolded proteins. The presence of PEG brushes and hydroxyl groups in the mixed micelle corona could interact with the molten globules of the refolding intermediates to facilitate the protein renaturation process. Three representative proteins, *i.e.,* GFP, lipase and lysozyme were utilized to demonstrate the good thermal protection efficiency. In addition, cell culture experiments indicated high cellular uptake efficiency and good biocompatibility of PEPS hybrid copolymers. When compared to numerous protein protection systems, which involve addition of various additives and tedious post-processing, the thermo-responsive hybrid PEPS self-assembled micelles developed in this paper could mimic the smart functionalities of a natural molecular

chaperone in a simple and spontaneous "capture and release" method using easy-controllable temperature as the sole trigger in an "on-demand" fashion.

5. Reference

1. W. Zhang and A. H. E. Muller, *Polymer*, 2010, **51**, 2133-2139.
2. K. Y. Mya, E. M. J. Lin, C. S. Gudipati, L. Shen and C. He, *J. Phys. Chem. B*, 2010, **114**, 9119-9127.
3. W. Zhang and A. H. E. Muller, *Macromolecules*, 2010, **43**, 3148-3152.
4. H. Hussain, B. H. Tan, C. S. Gudipati, Y. Xaio, Y. Liu, T. P. Davis and C. B. He, *J. Polym. Sci., Part A: Polym. Chem.*, 2008, **46**, 7287-7298.
5. X. J. Loh, Z.-X. Zhang, K. Y. Mya, Y.-l. Wu, C. B. He and J. Li, *J. Mater. Chem.*, 2010, **20**, 10634-10642.
6. B. H. Tan, H. Hussain and C. B. He, *Macromolecules*, 2011, **44**, 622-631.
7. M. A. Wahab, K. Y. Mya and C. He, *J. Polym. Sci., Part A: Polym. Chem.*, 2008, **46**, 5887-5896.
8. L. Ma, H. Geng, J. Song, J. Li, G. Chen and Q. Li, *J. Phys. Chem. B*, 2011, **115**, 10586-10591.
9. W. Zhang, B. Fang, A. Walther and A. H. E. Muller, *Macromolecules*, 2009, **42**, 2563-2569.
10. Z. Wang, B. Tan, H. Hussain and C. He, *Colloid Polym. Sci.*, 2013, **291**, 1803-1815.
11. W. Zhang, J. Yuan, S. Weiss, X. Ye, C. Li and A. H. E. MuÃàller, *Macromolecules*, 2011, **44**, 6891-6898.
12. K. Zeng, L. Wang and S. Zheng, *J. Phys. Chem. B*, 2009, **113**, 11831-11840.
13. H. Hussain, B. H. Tan, G. L. Seah, Y. Liu, C. B. He and T. P. Davis, *Langmuir*, 2010, **26**, 11763-11773.
14. S. Saeki, N. Kuwahara, M. Nakata and M. Kaneko, *Polymer*, 1976, **17**, 685-689.
15. V. G. De Bruijn, L. J. P. Van den Broeke, F. A. M. Leermakers and J. T. F. Keurentjes, *Langmuir*, 2002, **18**, 10467-10474.
16. K. Mortensen, W. Brown and E. Joergensen, *Macromolecules*, 1994, **27**, 5654-5666.
17. S. Walter and J. Buchner, *Angew. Chem., Int. Ed.*, 2002, **41**, 1098-1113.
18. X. Liu, Y. Liu, Z. Zhang, F. Huang, Q. Tao, R. Ma, Y. An and L. Shi, *Chem.- Eur. J.*, 2013, **19**, 7437-7442.
19. S. Ganguli, K. Yoshimoto, S. Tomita, H. Sakuma, T. Matsuoka, K. Shiraki and Y. Nagasaki, *J. Am. Chem. Soc.*, 2009, **131**, 6549-6553.
20. D. Rozema and S. H. Gellman, *J. Am. Chem. Soc.*, 1995, **117**, 2373-2374.
21. Y. Nomura, Y. Sasaki, M. Takagi, T. Narita, Y. Aoyama and K. Akiyoshi, *Biomacromolecules*, 2004, **6**, 447-452.
22. P. Štìpánek, in *Dynamic Light Scattering-The Method and Some Applications*, ed. D. Brown, Clarendon Press, Oxford, U.K.,, 1993, pp. 177-241.
23. B. Chu, *Laser light scattering: basic principles and practice (2nd)*, Academic Press, ISBN, 1991.
24. B. H. Zimm, *J. Chem. Phys.*, 1948, **16**, 1093-1099.
25. B. H. Zimm, *J. Chem. Phys.*, 1948, **16**, 1099-1116.
26. G. S. Waldo, B. M. Standish, J. Berendzen and T. C. Terwilliger, *Nat. Biotechnol.*, 1999, **17**, 691-695.
27. S. Sawada and K. Akiyoshi, *Macromol. Biosci.*, 2010, **10**, 353-358.
28. R. Ghaderi and J. Carlfors, *Pharm. Res.*, 1997, **14**, 1556-1562.
29. D. Pesce, Y. Wu, A. Kolbe, T. Weil and A. Herrmann, *Biomaterials*, 2013, **34**, 4360-4367.
30. Z. Li and J. Li, *J. Phys. Chem. B*, 2013, **117**, 14763-14774.
31. Z. Li, H. Yin, Z. Zhang, K. L. Liu and J. Li, *Biomacromolecules*, 2012, **13**, 3162-3172.
32. H. Hussain, B. H. Tan, G. L. Seah, Y. Liu, C. B. He and T. P. Davis, *Langmuir*, 2010, **26**, 11763-11773.

33. X. J. Loh, K. B. C. Sng and J. Li, *Biomaterials*, 2008, **29**, 3185-3194.
34. J. Pyun, K. Matyjaszewski, J. Wu, G.-M. Kim, S. B. Chun and P. T. Mather, *Polymer*, 2003, **44**, 2739-2750.
35. H. Tai, W. Wang, T. Vermonden, F. Heath, W. E. Hennink, C. Alexander, K. M. Shakesheff and S. M. Howdle, *Biomacromolecules*, 2009, **10**, 822-828.
36. Z. Li, Z. Zhang, K. L. Liu, X. Ni and J. Li, *Biomacromolecules*, 2012, **13**, 3977-3989.
37. Z. M. O. Rzaev, S. Dincer and E. Piskin, *Prog. Polym. Sci.*, 2007, **32**, 534-595.
38. E. S. Gil and S. M. Hudson, *Prog. Polym. Sci.*, 2004, **29**, 1173-1222.
39. X. Zhang, B. H. Tan and C. He, *Macromol. Rapid Commun.*, 2013, **34**, 1761-1766.
40. T. Kissel, Y. Li and F. Unger, *Adv. Drug Delivery Rev.*, 2002, **54**, 99-134.
41. Y. Einaga, *Prog. Polym. Sci.*, 1994, **19**, 1-28.
42. M. J. Hwang, J. M. Suh, Y. H. Bae, S. W. Kim and B. Jeong, *Biomacromolecules*, 2005, **6**, 885-890.
43. W. Peiqiang, M. Siddiq, C. Huiying, Q. Di and C. Wu, *Macromolecules*, 1996, **29**, 277-281.
44. W. Burchard, in *Light scattering : principles and development*, ed. W. Brown, Clarendon Press, Oxford, 1996, pp. 439-476.
45. Y. Xie and D. B. Wetlaufer, *Protein Sci.*, 1996, **5**, 517-523.
46. D. B. Wetlaufer and Y. Xie, *Protein Sci.*, 1995, **4**, 1535-1543.
47. X. J. Loh, S. H. Goh and J. Li, *Biomaterials*, 2007, **28**, 4113-4123.
48. G. H. Patterson, S. M. Knobel, W. D. Sharif, S. R. Kain and D. W. Piston, *Biophys. J.*, 1997, **73**, 2782-2790.

Scheme and Figures

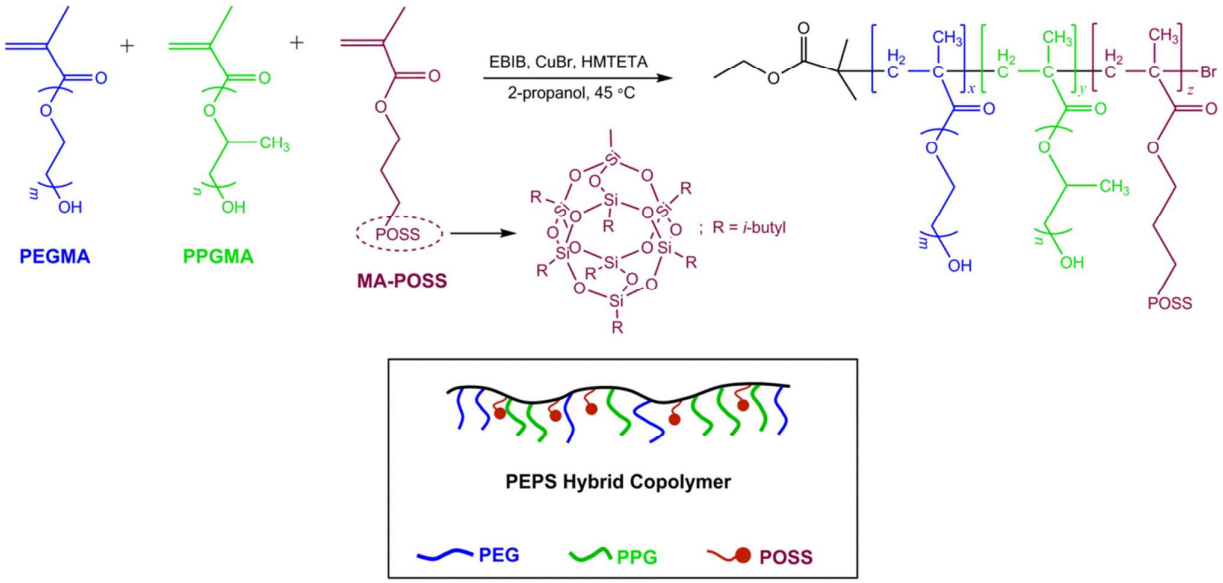

Scheme 1. Synthetic route and schematic illustration of poly(PEGMA-PPGMA-POSSMA) (PEPS) hybrid copolymers.

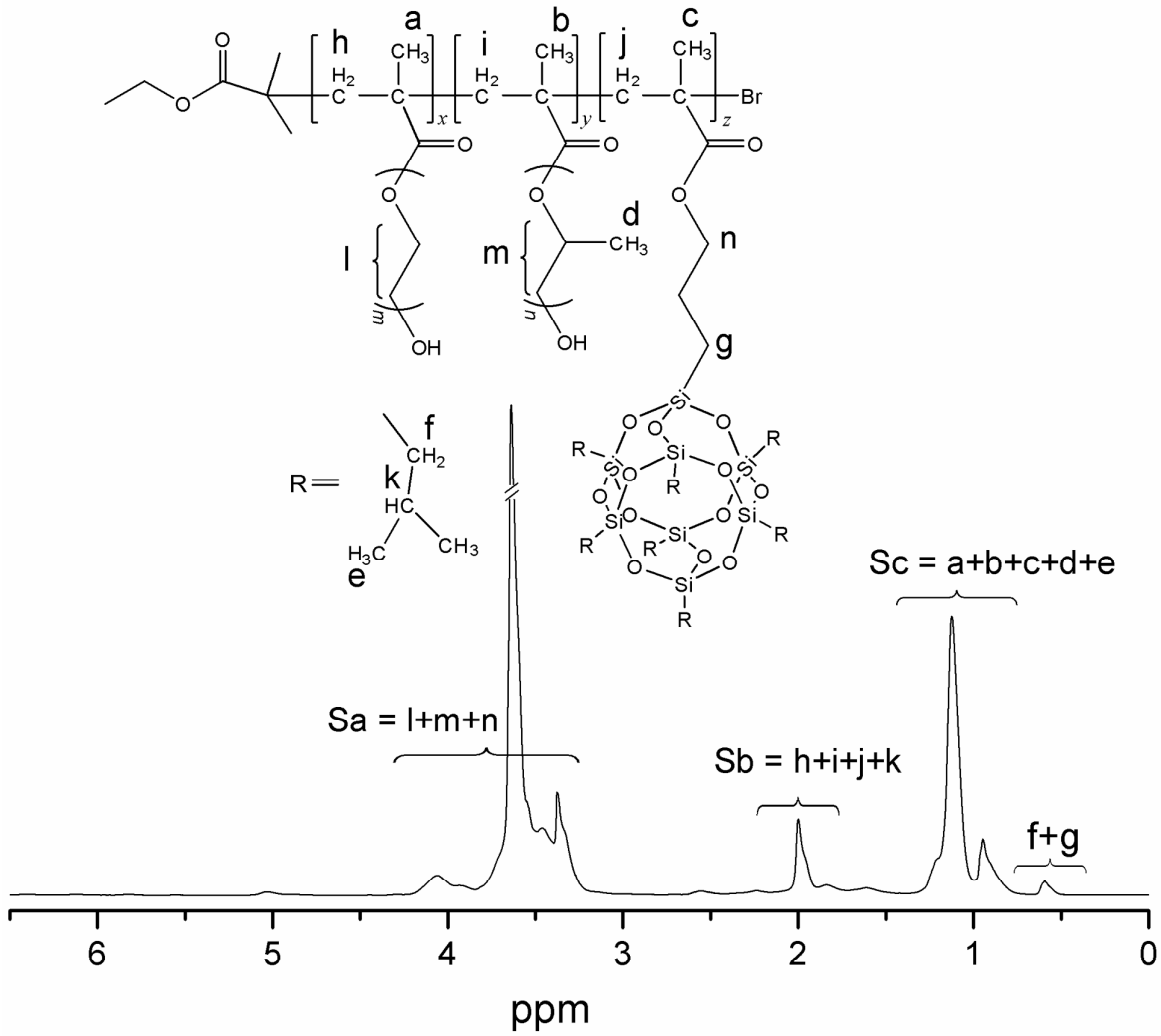

Fig. 1. ^{1}H NMR spectra of PEPS-3 hybrid copolymer in $CDCl_3$

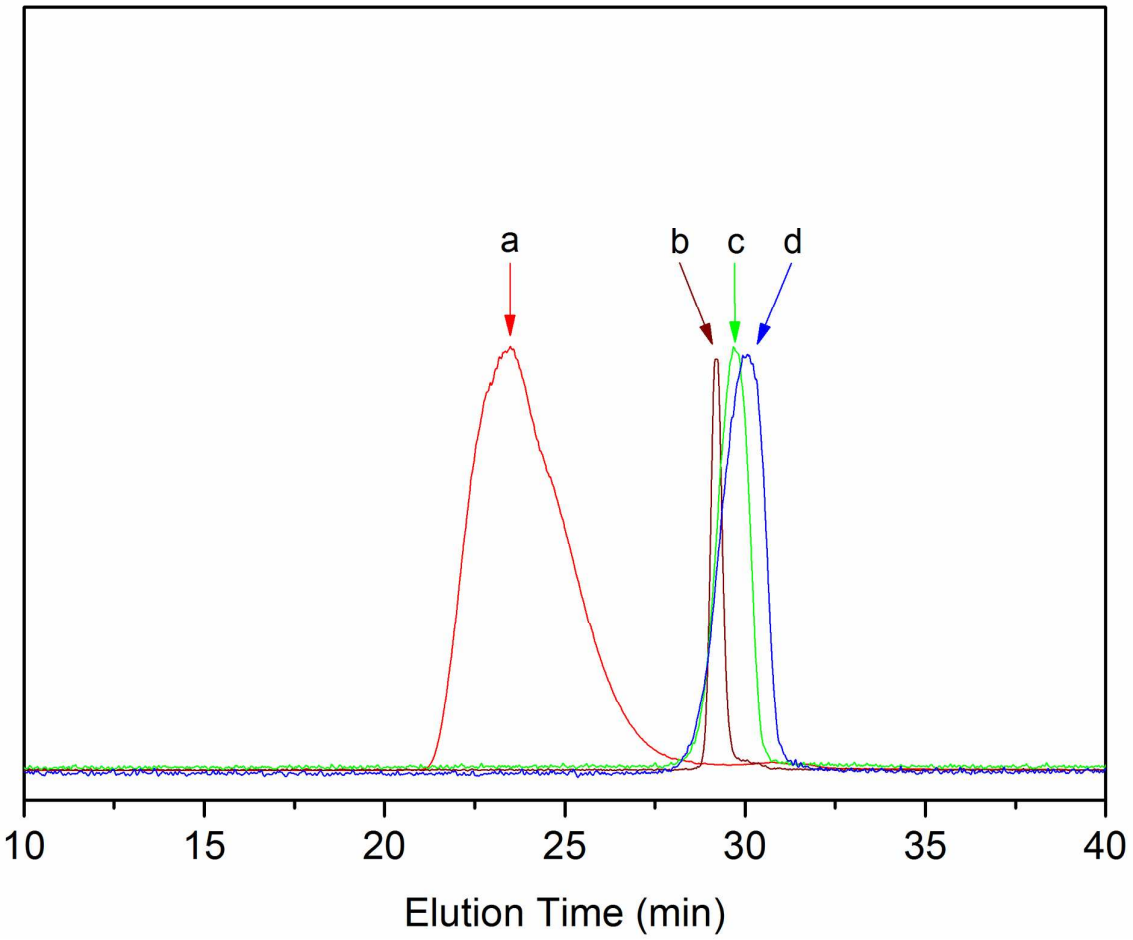

Fig. 2. GPC profiles of PEPS hybrid copolymer and its precursors. (a) PEPS-1; (b) POSSMA; (c) PPGMA375; and (d) PEGMA360.

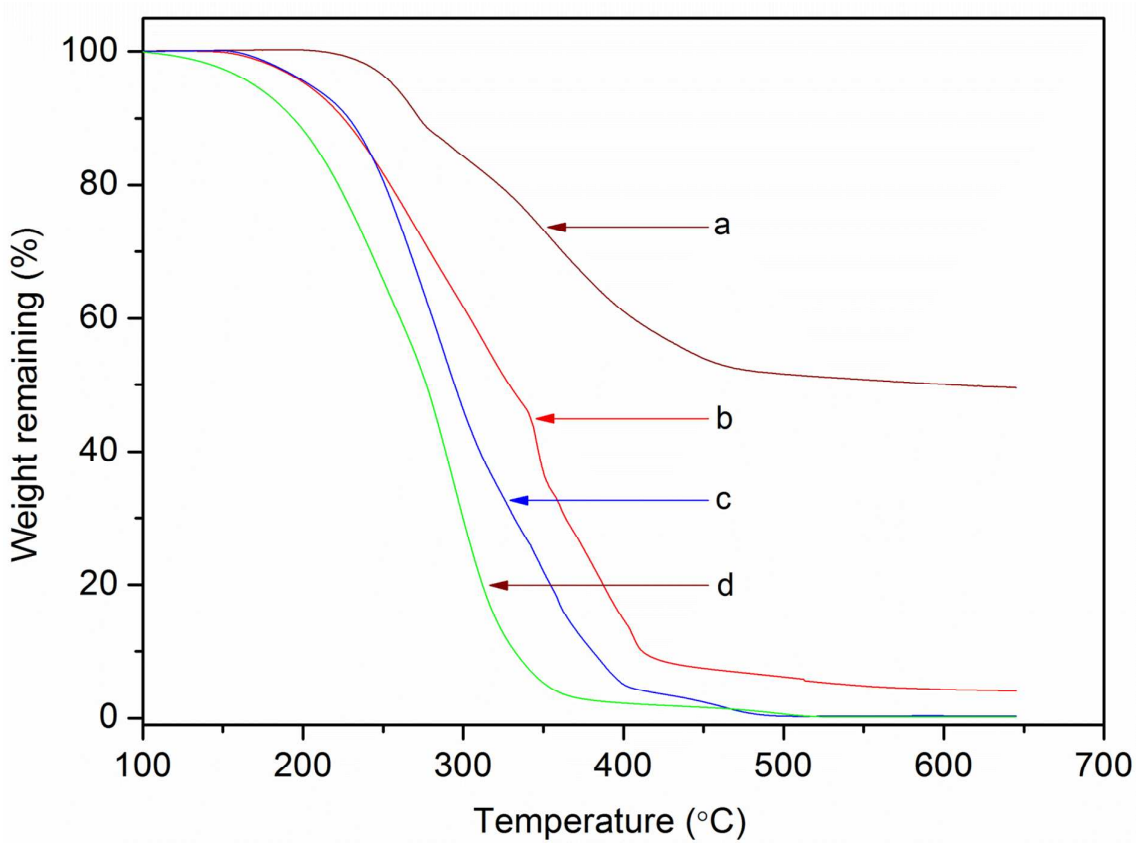

Fig. 3. TGA curves for (a) POSSMA; (b) PEPS-3; (c) PEGMA950; and (d) PPGMA375.

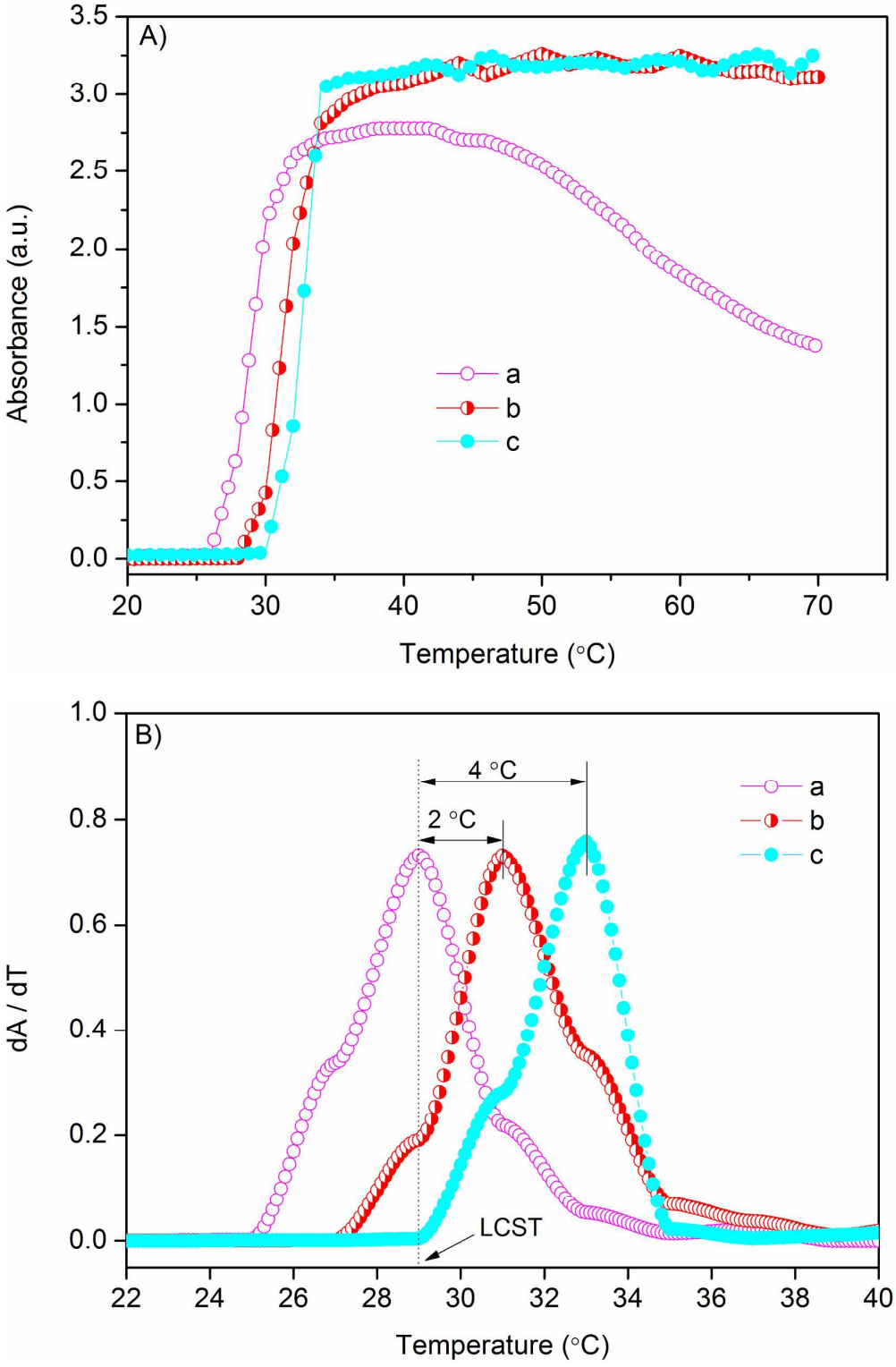

Fig. 4. (A) Thermo-responsive behaviours of PEPS hybrid copolymers in aqueous solutions (2.0 mg/mL), measured by UV-Vis spectroscopy at 530 nm; (B) LCST determination from the derivative absorbance spectroscopy. (a) PEP; (b) PEPS-1; (c) PEPS-2.

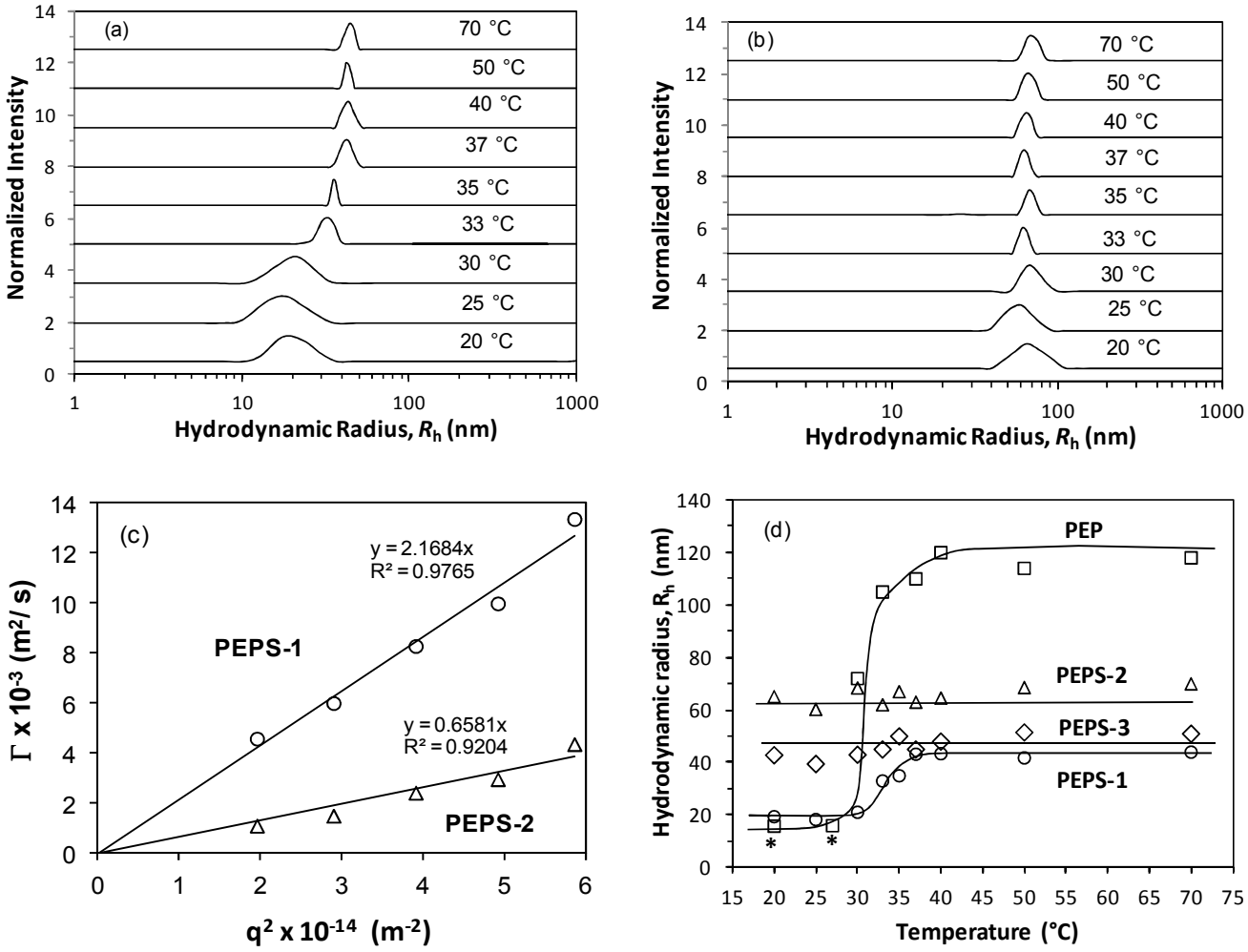

Fig. 5. Distribution of hydrodynamic radius, R_h of micelles in (a) PEPS-1 and (b) PEPS-2 for temperature ranging from 20°C to 70°C; (c) Dependence of decay rate Γ on q^2 for PEPS-1 (circle symbols) and PEPS-2 (triangle symbols) respectively at 25°C; (d) R_h of micelles as a function of solution temperature for PEP (square symbols), PEPS-1 (circle symbols), PEPS-2 (triangle symbols) and PEPS-3 (diamond symbols) respectively. The solid lines are included to guide the eye. All samples were prepared at polymer concentration of 0.5 mg/mL, except for PEP at temperatures below 30°C (copolymer concentration of 4 mg/mL, marked with an asterisk on the circle symbols) and PEPS-3 (copolymer concentration of 2 mg/mL). Measurements in (a), (b) and (d) were performed at scattering angle of 90° and R_h is calculated from Eq. (1).

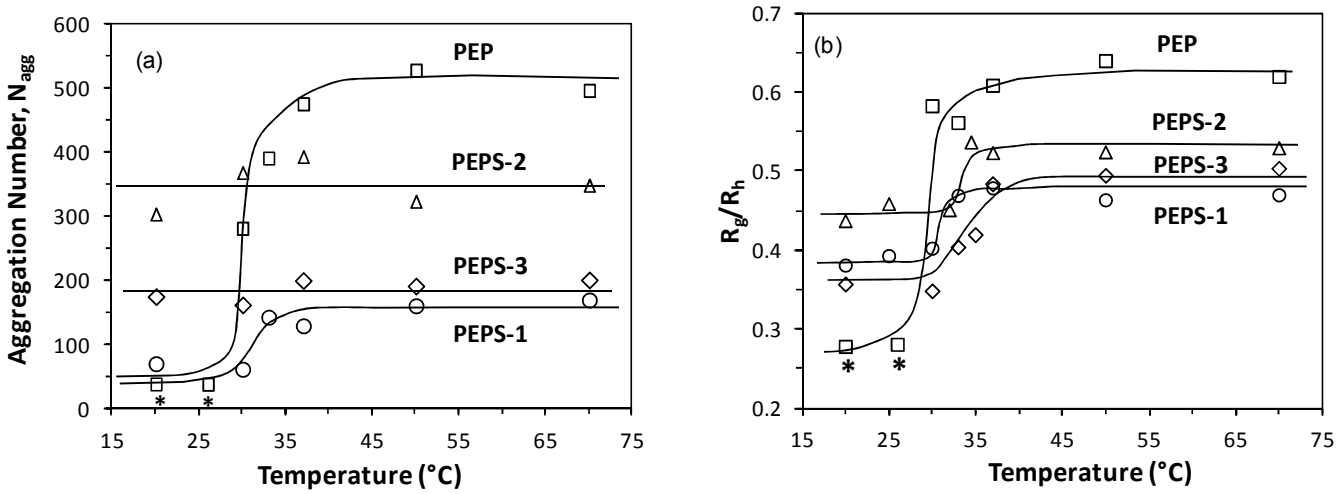

Fig. 6. (a) Aggregation number, N_{agg} and (b) dimensionless ratio R_g/R_h of aggregates in PEP and PEPS copolymers as a function of temperature determined from static light scattering (SLS) within the concentration range of 0.5 to 1.0 mg/mL except for PEP at temperatures below 30°C (concentration range of 3.5 to 4.5 mg/mL, marked with an asterisk on the square symbols) and PEPS-3 (copolymer concentration of 2.0 to 3.0 mg/mL). PEP, PEPS-1, PEPS-2 and PEPS-3 are represented by square, circle, triangle and diamond symbols respectively. The solid lines are drawn to guide the eye.

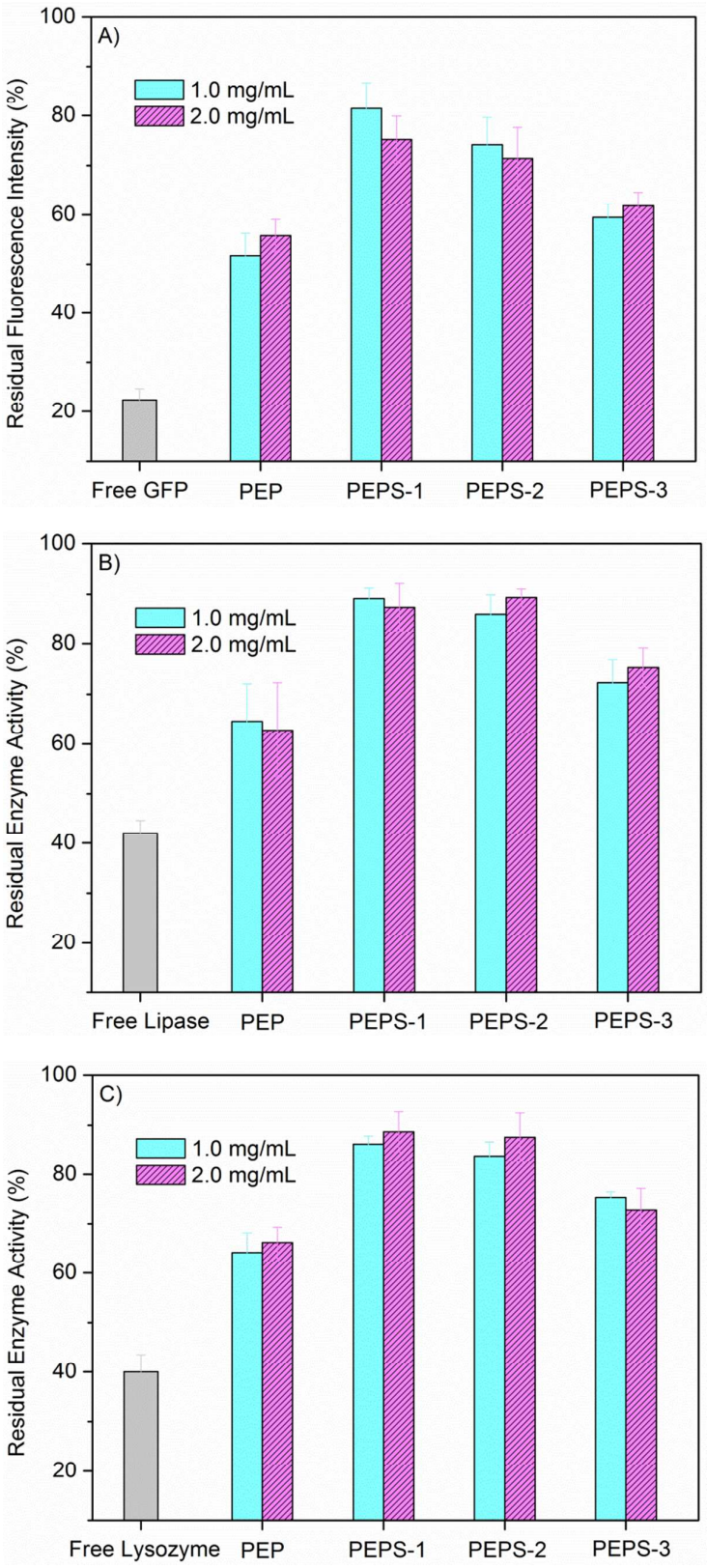

Fig. 7. Thermally denatured protein protection efficiencies for GFP (a), lipase (b) and lysozyme (c) in the presence of thermo-responsive PEPS hybrid copolymers.

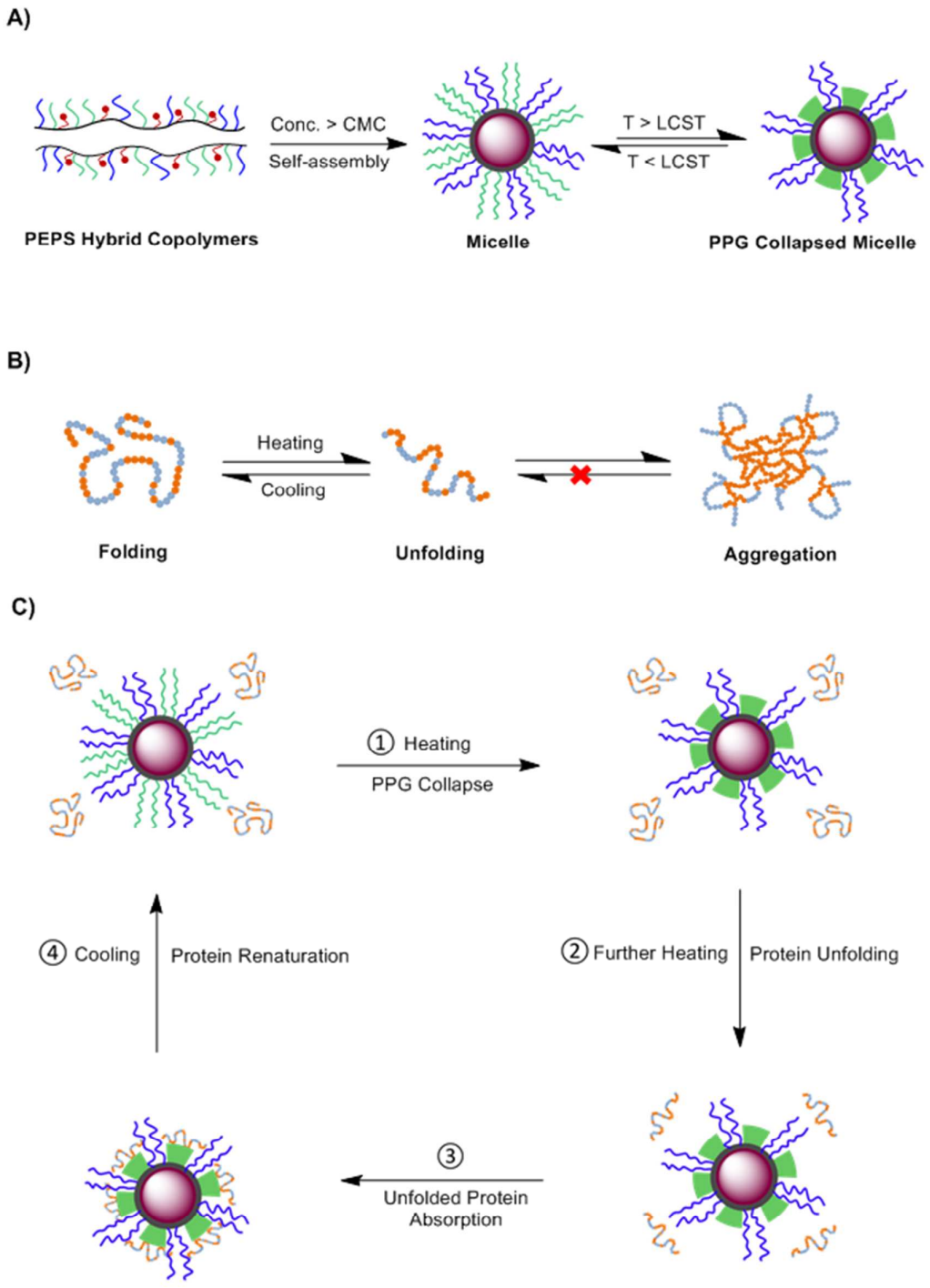

Fig. 8. Schematic representation of (A) thermo-responsive PEPS hybrid copolymer self-assembly in aqueous solution and (B) Heat-induced protein denaturation process. Yellow and light blue spots represent the hydrophobic and hydrophilic sites of proteins, respectively. (B) Proposed working mechanism of the thermally denatured protein protection by thermo-responsive PEPS hybrid micelles.

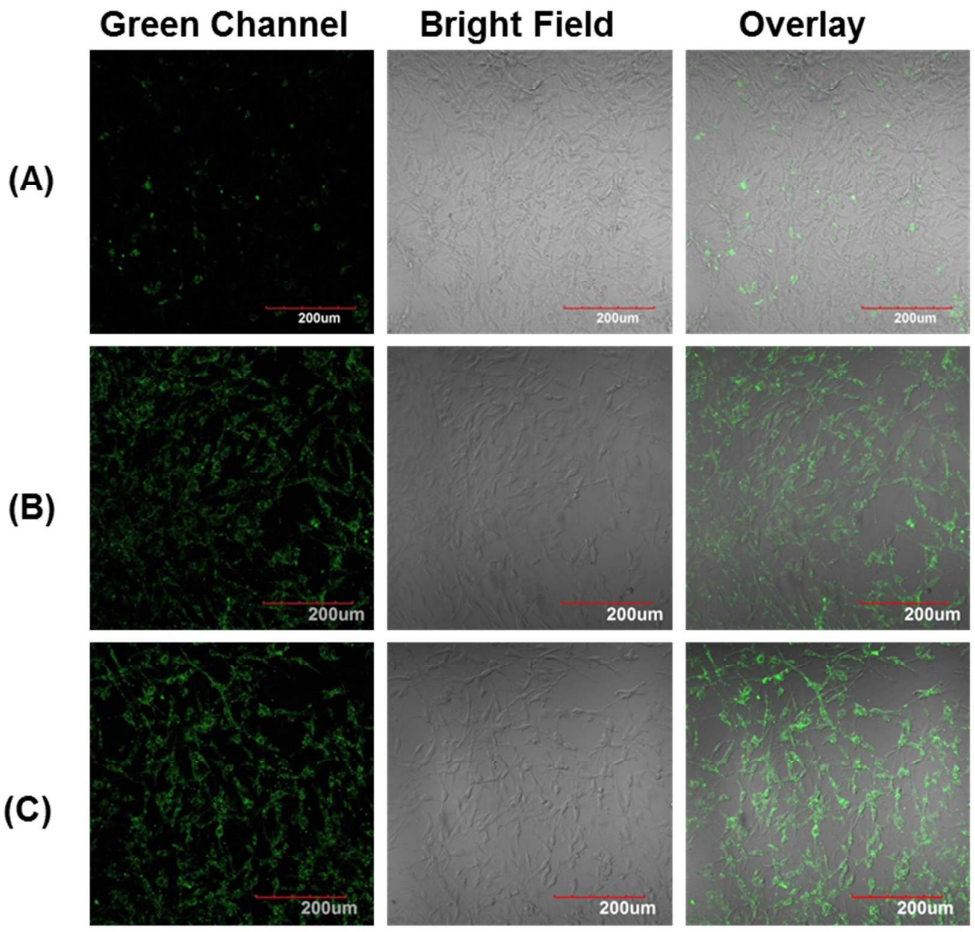

Fig. 9. The confocal microscopy images of C6 Glioma cells cultured with free GFP (A) and GFP with PEP copolymer (B) and PEPS hybrid copolymer (C).

Tables

Table 1. Molecular characteristics of PEPS hybrid copolymers and control polymer

Samples [a]	Copolymer composition in mole ratio				POSS (wt %) [c]	M_n ($\times 10^{-4}$) [d]	PDI [d]	LCST (ºC) [e]	CMC (mg/mL) [f]
	PEGMA360	PEGMA950	PPGMA375	POSSMA					
PEP	1.0 (1.0) [b]	0 (-)	2.0 (1.9)	0 (-)	-	2.56	1.5	29.0	3.0
PEPS-1	1.0 (1.0)	0 (-)	2.0 (1.5)	0.06 (0.04)	3.1	2.24	1.6	31.0	0.3
PEPS-2	1.0 (1.0)	0 (-)	2.0 (1.4)	0.18 (0.13)	6.7	2.01	1.5	33.0	0.1
PEPS-3	0 (-)	1.0 (1.0)	2.0/ (1.6)	0.18 (0.15)	6.3	2.31	1.4	-	1.0

[a] Hybrid copolymers poly(PEGMA-PPGMA-POSSMA) are denoted PEPS, where P represents poly-, E is for PEGMA, P for PPGMA, and S is for POSSMA.

[b] Feeding ratios of the starting materials in the reaction, the values in the parentheses show the mole ratios calculated from NMR results.

[c] Calculated from TGA thermograms.

[d] Determined from GPC.

[e] Determined by UV-Vis spectrophotometer.

[f] Determined by dynamic light scattering at 25 °C.

Table 2. DLS and SLS date for PEP and PEPS micelles only and the PEP/Lipase and PEPS/Lipase complexes under different solution temperatures

T (ºC)	LS parameters	Components							
		PEP only	PEP/ Lipase	PEPS-1 only	PEPS-1 /Lipase	PEPS-2 only	PEPS-2 /Lipase	PEPS-3 only	PEPS-3/ Lipase
25	R_h (nm)	16 ± 1	17 ± 2	18 ± 1	20 ± 1	60 ± 2	67 ± 3	40 ± 2	39 ± 2
	R_g (nm)	4.5 ± 0.3	4.9 ± 0.3	7.2 ± 0.3	7.6 ± 0.2	28 ± 1	32 ± 1	15 ± 1	14 ± 1
	R_g/R_h	0.28	0.29	0.39	0.38	0.46	0.48	0.37	0.36
37	R_h (nm)	110 ± 6	106 ± 6	43 ± 2	45 ± 2	63 ± 3	65 ± 2	45 ± 3	48 ± 3
	R_g (nm)	67 ± 4	68 ± 3	21 ± 1	22 ± 1	33 ± 2	35 ± 2	22 ± 1	24 ± 1
	R_g/R_h	0.61	0.64	0.48	0.49	0.52	0.54	0.48	0.50
70	R_h (nm)	118 ± 6	144 ± 7	44 ± 2	56 ± 2	70 ± 3	82 ± 3	51 ± 3	60 ± 3
	R_g (nm)	73 ± 4	99 ± 5	21 ± 1	36 ± 1	37 ± 2	62 ± 2	26 ± 2	37 ± 2
	R_g/R_h	0.62	0.69	0.47	0.64	0.53	0.75	0.50	0.61
25*	R_h (nm)	18 ± 1	18 ± 1	20 ± 1	24 ± 1	62 ± 3	66 ± 3	40 ± 2	52 ± 3
	R_g (nm)	4.9 ± 0.3	5.6 ± 0.3	8.0 ± 0.4	9.8 ± 0.4	29 ± 1	32 ± 1	16 ± 2	21 ± 2
	R_g/R_h	0.27	0.31	0.40	0.41	0.46	0.49	0.39	0.40

* Solutions were cooled to 25°C at ambient conditions after heating at 70°C